

ORIGINAL  
ARTICLEpISSN: 2384-3799 eISSN: 2466-1899  
Int J Thyroidol 2017 May 10(1): 14-23  
<https://doi.org/10.11106/ijt.2017.10.1.14>

# Ultrasonographic Evaluation of Diffuse Thyroid Disease: a Study Comparing Grayscale US and Texture Analysis of Real-Time Elastography (RTE) and Grayscale US

Jung Hyun Yoon<sup>1</sup>, Eunjung Lee<sup>2</sup>, Hye Sun Lee<sup>3</sup>, Eun-Kyung Kim<sup>1</sup>,  
Hee Jung Moon<sup>1</sup> and Jin Young Kwak<sup>1</sup>

Department of Radiology, Severance Hospital, Research Institute of Radiological Science, Yonsei University College of Medicine<sup>1</sup>,  
Department of Computational Science and Engineering, Yonsei University<sup>2</sup>, Department of Research Affairs, Biostatistics  
Collaboration Unit, Yonsei University College of Medicine<sup>3</sup>, Seoul, Korea

**Background and Objectives:** To evaluate and compare the diagnostic performances of grayscale ultrasound (US) and quantitative parameters obtained from texture analysis of grayscale US and elastography images in evaluating patients with diffuse thyroid disease (DTD). **Materials and Methods:** From September to December 2012, 113 patients (mean age, 43.4±10.7 years) who had undergone preoperative staging US and elastography were included in this study. Assessment of the thyroid parenchyma for the diagnosis of DTD was made if US features suggestive of DTD were present. Nine histogram parameters were obtained from the grayscale US and elastography images, from which 'grayscale index' and 'elastography index' were calculated. Diagnostic performances of grayscale US, texture analysis using grayscale US and elastography were calculated and compared. **Results:** Of the 113 patients, 85 (75.2%) patients were negative for DTD and 28 (24.8%) were positive for DTD on pathology. The presence of US features suggestive of DTD showed significantly higher rates of DTD on pathology, 60.7% to 8.2% ( $p<0.001$ ). Specificity, accuracy, and positive predictive value was highest in US features, 91.8%, 84.1%, and 87.6%, respectively (all  $ps<0.05$ ). Grayscale index showed higher sensitivity and negative predictive value (NPV) than US features. All diagnostic performances were higher for grayscale index than the elastography index. Area under the curve of US features was the highest, 0.762, but without significant differences to grayscale index or mean of elastography (all  $ps>0.05$ ). **Conclusion:** Diagnostic performances were the highest for grayscale US features in diagnosis of DTD. Grayscale index may be used as a complementary tool to US features for improving sensitivity and NPV.

**Key Words:** Thyroid, Ultrasound, Diffuse thyroid disease, Elastography, Texture analysis

## Introduction

Ultrasonography (US) is an easy, safe, and accurate imaging modality that is widely used for lesion detection, differential diagnosis, and for biopsy under imaging-guidance in various nodular diseases of the

thyroid gland. Adding to nodule characterization, grayscale US features such as changes in parenchymal echogenicity, anteroposterior diameter or vascularity, coarse echotexture, and the presence of marginal nodularity has been reported to be helpful in the evaluation of diffuse thyroid disease (DTD).<sup>1-4)</sup> But while these grayscale US features may suggest the

Received October 20, 2016 / Revised February 9, 2017 / Accepted February 9, 2017

Correspondence: Jin Young Kwak, MD, Department of Radiology, Severance Hospital, Research Institute of Radiological Science, Yonsei University College of Medicine, 50 Yonsei-ro, Seodaemun-gu, Seoul 03722, Korea  
Tel: 82-2-2228-7400, Fax: 82-2-393-3035, E-mail: docjin@yuhs.ac

Copyright © 2017, the Korean Thyroid Association. All rights reserved.

© This is an open-access article distributed under the terms of the Creative Commons Attribution Non-Commercial License (<http://creativecommons.org/licenses/by-nc/4.0/>), which permits unrestricted non-commercial use, distribution, and reproduction in any medium, provided the original work is properly cited.

presence of DTD, this has its limitations in that it provides morphologic features only, and cannot reflect the intrinsic changes secondary to the disease course of DTD.

Effort has been made in obtaining additional information other than the morphologic features that can be used in lesion characterization, either using advanced technology or software. For example, elastography is nowadays popularly used which provides the intrinsic stiffness properties of the targeted tissue.<sup>5–7)</sup> Another example is texture analysis of US images, which is a technique that calculates the parameters computed from the distribution of pixels characterizing texture type and the underlying structure of objects shown in an obtained image.<sup>8)</sup> These methods have been applied in characterization of masses of various origin, based on the concept that the additional information obtained enables more precise lesions characterization, therefore, mostly used in differentiating between benign and malignant lesions.<sup>6,7,9–13)</sup> Both elastography and texture analysis of grayscale US may also be applied in the evaluation of DTD, and considering the quantitative values obtained from both methods, these may be a more objective analytic method in evaluating DTD compared to analyzing US features. A few studies have applied quantitative analysis based on texture analysis of grayscale US, real-time elastography (RTE), and shearwave elastography (SWE) in the evaluating of DTD.<sup>2,14–18)</sup> However, there were no studies that compared the diagnostic performances between texture analysis of elastography and grayscale US.

Based on this, we evaluated and compared the diagnostic performances using grayscale US features, quantitative parameters obtained from texture analysis of grayscale US and elastography images in evaluating patients with DTD.

## Materials and Methods

This study is of a retrospective design, and has been approved by our Institutional Review Board (IRB). Neither patient approval nor informed consent was required for review of medical records or images.

Signed informed consent was obtained from all patients prior to biopsy or surgical procedures.

### Patients

From September to December 2012, 115 patients had undergone preoperative staging US and subsequent elastography at our institution. Among these patients, 2 were excluded due to the following reasons: the lack of sufficient amount of thyroid parenchyma for analysis as the entire thyroid gland was nearly replaced with multiple nodules ( $n=1$ ) and technical problems in obtaining quantitative parameters from elastography ( $n=1$ ). A total of 113 patients were included in this study. Mean age of the patients was  $43.4 \pm 10.7$  years (range, 23 to 66 years). Among the 113 patients, 93 (82.3%) were women and 20 (17.7%) were men.

All 113 nodules were included in our previous article which evaluated the diagnostic performances of quantitative histogram parameters using RTE in the diagnosis of patients with DTD.<sup>14)</sup>

### Grayscale US and Real-Time Elastography

US examinations were performed using a 5– to 13-MHz linear array transducer (HI VISION Ascendus, Hitachi Aloka Medical, Tokyo, Japan). Preoperative staging US was performed by one of the three board-certified radiologists (H.J.M., J.Y.K., and E-K.K) with 8 to 16 years of experience in thyroid imaging. During grayscale US examinations, assessment of the thyroid parenchyma for the diagnosis of DTD was made and recorded prospectively based on the presence of the following US features: changes in parenchymal echogenicity, vascularity or anteroposterior diameter of the thyroid gland, coarse echotexture, presence of marginal nodularity, and the presence of scattered microcalcifications.<sup>1,2)</sup>

After grayscale US examinations, real-time elastography was performed by the same radiologist. All elastography images were obtained in a longitudinal plane, with the probe positioned perpendicular to the skin. Light, repetitive compression forces were applied with the probe to obtain elastography images. Images were displayed in a split-screen mode with elastog-

raphy images superimposed on the corresponding grayscale images on the left, and grayscale US images on the right. Each pixel of the elastography image was displayed in one of 256 colors, ranging from blue (indicating no strain) to red (indicating greatest strain). Patients were asked to refrain from speaking or swallowing during image acquisition. A region-of-interest (ROI) was set to include a sufficient amount of thyroid parenchyma, consisting more than one-third of a thyroid lobe, excluding thyroid nodules.

### Texture Analysis from Grayscale US and Elastography

Grayscale US and elastography images of the thyroid parenchyma were saved as 8-bit bmp images from our picture archiving and communication system (PACS). For histogram and co-occurrence matrix analysis of both grayscale US and elastography images, we used an in-house software developed with Matlab R2010a (MathWorks, Natick, MA, USA) (Fig. 1). One longitudinal elastographic image was selected for texture analysis. Images are automatically displayed in

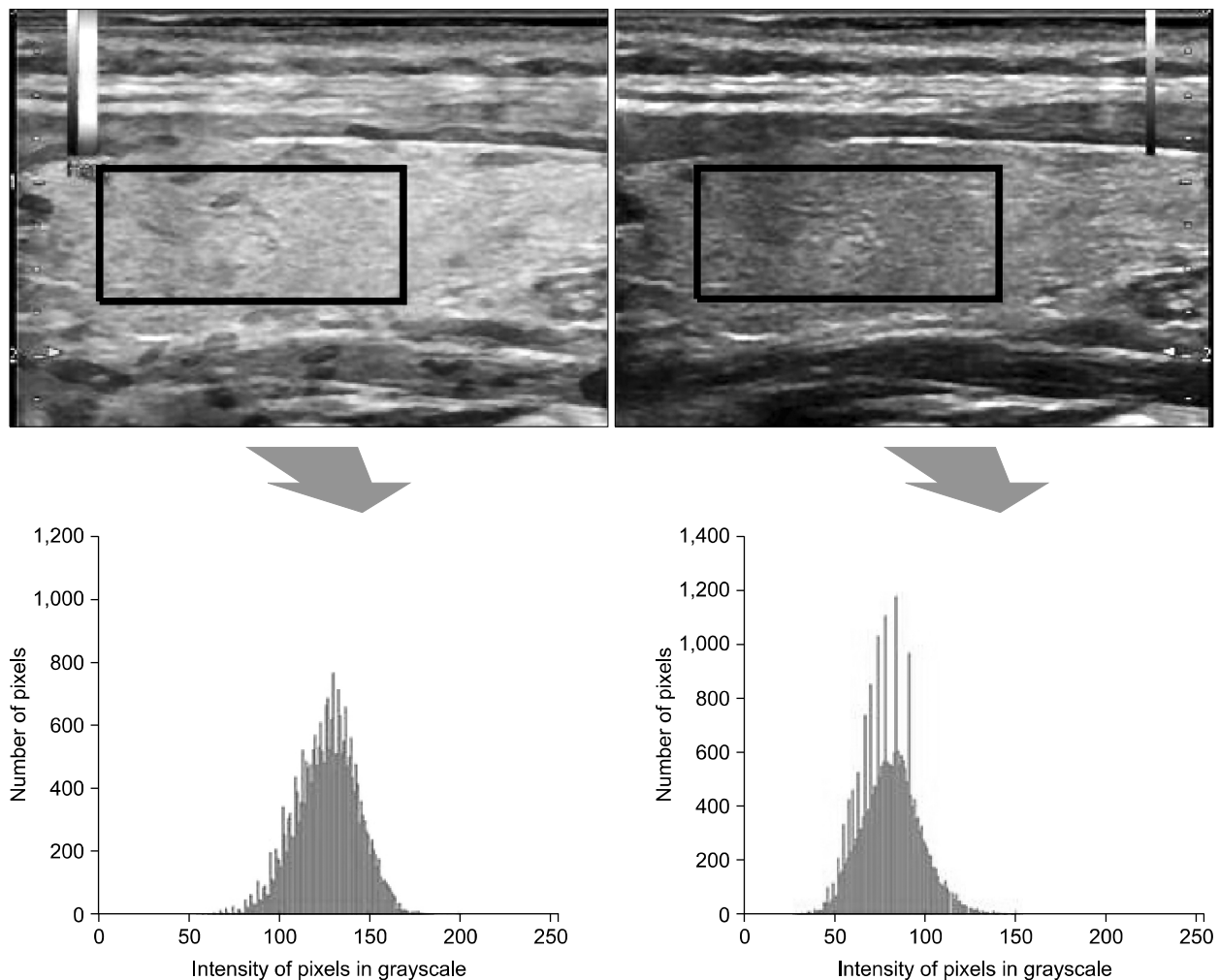


**Fig. 1.** Example of texture analysis of elastography and grayscale US. One longitudinal elastographic image was selected for texture analysis. Images are automatically displayed in split-screen mode to show both gray-scale US and corresponding color-scale elastographic images. A region of interest (ROI) was previously set on the elastography by the radiologist who performed US (left, upper row, box). The same ROI was set on the grayscale US (right, upper row, box) transferring from elastographic ROI. From these ROIs, histogram and cooccurrence matrix parameters are automatically calculated with an in-house built software. Histogram analysis (bottom row) show the distribution of the number pixels (y-axis) according to the pixel intensity value (x-axis) within the ROIs.

split-screen mode to show both gray-scale US and corresponding color-scale elastographic images. An ROI was previously set on the elastography by the radiologist who performed US (upper row). The same ROI was set on the grayscale US (right, middle row) transferring from elastographic ROI (left, middle row). From these ROIs, histogram and co-occurrence matrix parameters are automatically calculated with software. Histograms of elastography and grayscale US showed distribution of number of pixels (y-axis) according to pixel intensity value within the ROIs. Pixel intensity values in an ROI were measured ranging from 0 (black on gray-scale) to 256 (white on gray-scale). Co-occurrence matrix were calculated with diagonal direction and interpixel distance of 1. Four histogram parameters were obtained from the grayscale US images as the following: mean, standard deviation, skewness, and kurtosis. Five co-occurrence matrix parameters were obtained from the elastography images as the following: contrast, correlation, uniformity, homogeneity, and entropy.<sup>19)</sup>

Mean is defined as the average relative value of pixel intensity within the ROI classified in 256 scales. Standard deviation refers to how far or how often an outcome will deviate from the average value. Skewness is the scale of asymmetry of which its statistical value indicates to what degree a symmetric object of the histogram is skewed. Kurtosis is used as the peakedness of which its statistical value indicates if a histogram distribution can be concentrated into an average value. Contrast indicates the feature value of the textural variations. Correlation is the feature value of the textural directivity. Uniformity is the feature value of textural uniformity, and homogeneity is of textural homogeneity. Entropy indicates the feature value of the texture randomness.

### Histopathological Analysis

The classification regarding DTD was made based on the pathological reports after surgery. The pathologic criteria for thyroiditis at our institution include the presence of lymphocytic and plasma cell infiltrates, oxyphilic cells, formation of lymphoid follicles with germinal centers and atrophic changes of thyroid

tissues.<sup>14,20)</sup> The inclusion of pathologic diagnosis of lymphocytic thyroiditis or diffuse hyperplasia was considered positive for DTD, while if there was no mention of lymphocytic thyroiditis in pathology reports, they were considered negative for DTD.

### Statistical Analysis

Clinicopathological features were compared between patients positive for DTD and negative for DTD. In the analysis using the presence of US features in evaluating DTD, patients were considered negative on US if there were no US features present while they were considered positive on US when 1 or more US features were visualized. Chi-square test was used in comparison for categorical variables. Independent two-sample t-test was used in comparison of continuous variables.

Because of data clustering, principal component analysis (PCA) was performed to identify the linear combination of the 9 parameters obtained from texture analysis of grayscale US and elastography. PCA revealed three principal components with eigen values  $\geq 1.0$  for grayscale US, and two principal components with eigen values  $\geq 1.0$  for elastography. Using the principal components in an integrative formula, functional scores for grayscale US, i.e., grayscale index, and elastography, i.e., elastography index was calculated.<sup>14,21)</sup> Diagnostic performances including sensitivity, specificity, accuracy, positive predictive value (PPV), and negative predictive value (NPV) of grayscale US features, texture analysis parameters of grayscale US and elastography were calculated using the cutoff values defined for each parameter according to the Youden index and compared using generalized estimating equation (GEE) method. Area under the receiver operating characteristics (ROC) curve (AUC) values were calculated and compared using DeLong method.

P value of less than 0.05 was considered to indicate significant difference. Analysis was performed using SAS software (version 9.2, SAS, Cary, NC, USA).

## Results

Based on the pathology reports, 85 (75.2%) patients were negative for DTD and 28 (24.8%) were positive for DTD. Mean age of the patients who were positive for DTD ( $45.7 \pm 10.8$  years) was older than patients who were negative for DTD ( $42.7 \pm 10.7$  years), but without statistical significance ( $p=0.203$ ). Women had more frequent rates of positive for DTD than men, 96.4% to 3.6% ( $p=0.023$ ).

Table 1 summarizes the comparison of parameters between patients positive for DTD to patients negative for DTD. The presence of US features suggestive of DTD showed significantly higher rates of DTD on pathology, 60.7% to 8.2% ( $p<0.001$ ). Among the parameters derived from texture analysis of grayscale US, correlation and entropy were significantly higher in patients positive for DTD,  $0.739 \pm 0.039$  to  $0.717 \pm 0.059$  and  $1.116 \pm 0.121$  to  $1.037 \pm 0.190$ , respectively ( $p=0.026$  and  $0.013$ , respectively). Uniformity

was significantly lower in patients positive for DTD,  $0.466 \pm 0.069$  to  $0.506 \pm 0.106$  ( $p=0.024$ ). Of the parameters derived from elastography, mean was significantly lower in patients positive for DTD,  $165.2 \pm 14.9$  to  $172.5 \pm 10.5$  ( $p=0.021$ ).

For parameters from texture analysis of grayscale US, characteristic root values ( $\lambda$ ) of anterior three main functions are 4,342, 1,952, and 1,136, dedication rates are 48.2%, 21.7%, and 12.6%, respectively. According to PCA, three principal components with eigen values  $\geq 1$  were chosen to formulate the integrative function as follows (cumulative dedication rate: 82.6%).

### Principle component1:

$$0.207 \times \text{Mean} + 0.346 \times \text{Standard deviation} + 0.009 \times \text{Skewness} + 0.009 \times \text{Kurtosis} + 0.415 \times \text{Contrast} + 0.249 \times \text{Correlation} - 0.455 \times \text{Uniformity} - 0.415 \times \text{Homogeneity} + 0.473 \times \text{Entropy}$$

### Principle component2:

$$-0.465 \times \text{Mean} + 0.354 \times \text{Standard deviation} + 0.191 \times \text{Skewness} - 0.296 \times \text{Kurtosis} - 0.312 \times \text{Contrast} +$$

**Table 1.** Comparison of US features, grayscale US and RTE parameters according to the presence of DTD

	Negative for DTD (n=85)	Positive for DTD (n=28)	p
<i>Gray scale US</i>			
Negative on US	78 (91.8%)	11 (39.3%)	<0.001
Positive on US	7 (8.2%)	17 (60.7%)	
<i>Texture analysis of gray scale US</i>			
Mean	79.6±13.7 (46.4, 112.9)	77.1±14.4 (52.3, 115.6)	0.408
SD	14.3±2.4 (9.7, 23.5)	15.0±1.9 (11.5, 19.5)	0.127
Skewness	0.2±0.3 (−0.8, 1.0)	0.3±0.3 (−0.5, 1.0)	0.157
Kurtosis	4.0±1.4 (2.3, 11.6)	4.1±1.2 (2.6, 7.2)	0.909
Contrast	0.1±0.01 (0.1, 0.2)	0.1±0.02 (0.1, 0.2)	0.209
Correlation	0.717±0.059 (0.589, 0.838)	0.739±0.039 (0.660, 0.799)	0.026
Uniformity	0.506±0.106 (0.302, 0.805)	0.466±0.069 (0.354, 0.618)	0.024
Homogeneity	0.94±0.01 (0.91, 0.97)	0.94±0.01 (0.92, 0.95)	0.174
Entropy	1.037±0.190 (0.507, 1.562)	1.116±0.121 (0.854, 1.291)	0.013
<i>Texture analysis of RTE</i>			
Mean	172.5±10.5 (151.8, 198.6)	165.2±14.9 (130.1, 195.7)	0.021
SD	46.9±5.8 (33.1, 65.8)	47.6±6.6 (33.5, 60.4)	0.578
Skewness	−1.2±0.6 (−2.7, −0.4)	−1.2±0.5 (−2.3, −0.4)	0.775
Kurtosis	7.9±2.7 (3.7, 17.7)	7.3±2.8 (2.3, 14.7)	0.400
Contrast	0.7±0.2 (0.4, 1.2)	0.7±0.2 (0.5, 1.2)	0.237
Correlation	0.770±0.052 (0.636, 0.872)	0.788±0.060 (0.7, 0.9)	0.111
Uniformity	0.263±0.052 (0.185, 0.398)	0.259±0.056 (0.145, 0.383)	0.692
Homogeneity	0.900.02 (0.86, 0.93)	0.90±0.01 (0.88, 0.93)	0.879
Entropy	1.839±0.193 (1.395, 2.248)	1.891±0.204 (1.448, 2.347)	0.230

DTD: diffuse thyroid disease, RTE: real-time elastography, SD: standard deviation, US: ultrasound  
Minimum and maximum values are in parentheses.

**Table 2.** Diagnostic performances of US features, grayscale US and RTE parameters in the diagnosis of DTD

	Cutoff	Sensitivity	p	Specificity	p	Accuracy	p	PPV	p	NPV	p	A <sub>z</sub> (95% CI)	p*
<i>Gray scale US</i>	–	60.7 (17/28)	–	91.8 (78/85)	–	84.1 (95/113)	–	70.8 (17/24)	–	87.6 (78/89)	–	0.762 (0.666, 0.860)	–
<i>Texture analysis of gray scale US</i>													
Mean	≤86.9	85.7 (24/28)	0.005 <sup>†</sup> 0.705*	29.4 (25/85)	<0.001 <sup>†</sup> <0.001*	43.4 (49/113)	0.002 <sup>†</sup> 0.002*	28.6 (24/84)	<0.001 <sup>†</sup> 0.241*	86.2 (25/29)	0.316 <sup>†</sup> 0.444*	0.558 (0.433, 0.683)	0.108 <sup>†</sup> 0.264*
SD	>13.9	78.6 (22/28)	0.067*	49.4 (42/85)	0.053*	56.6 (64/113)	0.368*	33.9 (22/65)	0.881*	87.5 (42/48)	0.187*	0.632 (0.517, 0.747)	0.403*
Skewness	>0.3	57.1 (16/28)	0.005*	64.7 (55/85)	–	62.8 (71/113)	–	34.8 (16/46)	–	82.1 (55/67)	0.079*	0.585 (0.459, 0.711)	0.363*
Kurtosis	>3.8	53.6 (15/28)	0.002*	57.6 (49/85)	0.270*	56.6 (63/113)	0.260*	29.4 (15/51)	0.336*	79.0 (49/62)	0.032*	0.530 (0.402, 0.658)	0.133*
Contrast	>1	71.4 (20/28)	0.014*	48.2 (41/85)	0.023*	54.0 (61/113)	0.178*	31.3 (20/64)	0.576*	83.7 (41/49)	0.048*	0.582 (0.469, 0.694)	0.084*
Correlation	>0.7	85.7 (24/28)	0.654*	45.9 (39/85)	0.010*	55.8 (63/113)	0.274*	34.3 (24/70)	0.930*	90.7 (39/43)	0.783*	0.624 (0.516, 0.731)	0.485*
Uniformity	≤0.5	85.7 (24/28)	0.309*	41.2 (35/85)	0.001*	52.2 (59/113)	0.105*	32.4 (24/74)	0.681*	89.8 (35/39)	0.321*	0.604 (0.493, 0.716)	0.080*
Homogeneity	≤0.9	71.4 (20/28)	0.014*	49.4 (42/85)	0.037*	54.9 (62/113)	0.230*	31.8 (20/63)	0.635*	84.0 (42/50)	0.054*	0.586 (0.473, 0.670)	0.105*
Entropy	>1.0	89.3 (25/28)	>0.999*	40.0 (34/85)	<0.001*	52.2 (59/113)	0.105*	32.9 (25/76)	0.734*	91.9 (34/37)	0.581*	0.640 (0.529, 0.751)	0.180*
Grayscale index	> –0.3	89.3 (25/28)	–	41.2 (35/85)	0.001*	53.1 (60/113)	0.134*	33.3 (25/75)	0.794*	92.1 (35/38)	–	0.661 (0.554, 0.769)	–
<i>Texture analysis of RTE</i>													
Mean	≤167.7	60.7 (17/28)	0.002 <sup>†</sup> 0.002*	65.9 (56/85)	0.244 <sup>†</sup> <0.001*	64.6 (73/113)	0.057 <sup>†</sup> 0.039*	37.0 (17/46)	0.074 <sup>†</sup> 0.108*	83.6 (56/67)	0.584 <sup>†</sup> 0.242*	0.645 (0.525, 0.766)	–
SD	>51.7	32.1 (9/28)	<0.001*	82.4 (70/85)	0.314*	70.0 (79/113)	0.158*	37.5 (9/24)	0.154*	78.7 (70/89)	0.034*	0.540 (0.409, 0.671)	0.251*
Skewness	≤ –0.9	78.6 (22/28)	0.142*	34.1 (29/85)	<0.001*	45.1 (51/113)	<0.001*	28.2 (22/78)	0.020*	82.9 (29/35)	0.326*	0.490 (0.368, 0.612)	0.077*
Kurtosis	≤5.6	28.6 (8/28)	<0.001*	87.1 (74/85)	>0.999*	72.6 (82/113)	0.315*	42.1 (8/19)	0.283*	78.7 (74/94)	0.035*	0.546 (0.415, 0.678)	0.242*
Contrast	≤0.6	42.9 (12/28)	<0.001*	80.0 (68/85)	0.152*	70.8 (80/113)	0.218*	41.4 (12/29)	0.239*	81.0 (68/84)	0.147*	0.612 (0.487, 0.737)	0.648*
Correlation	>0.8	42.9 (12/28)	<0.001*	87.1 (74/85)	–	76.1 (86/113)	–	52.2 (12/23)	–	82.2 (74/90)	0.116*	0.577 (0.441, 0.713)	0.438*

Table 2. Continued

	Cutoff	Sensitivity	p	Specificity	p	Accuracy	p	PPV	p	NPV	p	A <sub>z</sub> (95% CI)	p*
Uniformity	>0.2	75.0 (21/28)	0.079*	37.7 (32/85)	<0.001*	46.9 (53/113)	<0.001*	28.4 (21/74)	0.020*	82.1 (32/39)	0.276*	0.510 (0.385, 0.635)	0.141*
Homogeneity	≤0.9	92.9 (26/28)	–	24.7 (21/85)	<0.001*	41.6 (47/113)	<0.001*	28.9 (26/90)	0.009*	91.3 (21/23)	–	0.523 (0.406, 0.640)	0.130*
Entropy	>1.8	82.1 (23/28)	0.067*	32.9 (28/85)	<0.001*	45.1 (51/113)	<0.001*	28.8 (23/80)	0.006*	84.9 (28/33)	0.206*	0.548 (0.423, 0.665)	0.211*
Elastography index	> -1.1	85.7 (24/28)	0.142*	28.2 (24/85)	<0.001*	42.5 (48/113)	<0.001*	28.2 (24/85)	0.006*	85.7 (24/28)	0.241*	0.515 (0.394, 0.633)	0.138*

A<sub>z</sub>: area under the receiver operating characteristics curve, CI: confidence interval, DTD: diffuse thyroid disease, RTE: real-time elastography, SD: standard deviation, US: ultrasound  
Raw data are in parentheses

\*p values compared to the highest value within each modality.

†p values compared to US features, using the parameter showing highest value.

$0.568 \times \text{Correlation} - 0.079 \times \text{Uniformity} + 0.307 \times \text{Homogeneity} + 0.114 \times \text{Entropy}$

*Principle component3:*

$-0.187 \times \text{Mean} - 0.004 \times \text{Standard deviation} + 0.788 \times \text{Skewness} + 0.576 \times \text{Kurtosis} + 0.076 \times \text{Contrast} - 0.032 \times \text{Correlation} + 0.041 \times \text{Uniformity} - 0.064 \times \text{Homogeneity} - 0.007 \times \text{Entropy}$

*Grayscale Index* =  $(4.342 \times \text{Prin1} + 1.952 \times \text{Prin2} + 1.136 \times \text{Prin3})/9$

For parameters from elastography, characteristic root values ( $\lambda$ ) of anterior two main functions are 5.304 and 1.937, dedication rates are 58.9% and 21.5%, respectively. According to PCA, two principal components with eigen values  $\geq 1$  were chosen to formulate the integrative function as follows (cumulative dedication rate: 80.5%).

*Principle component1:*

$0.045 \times \text{Mean} + 0.404 \times \text{Standard deviation} + 0.337 \times \text{Skewness} - 0.409 \times \text{Kurtosis} + 0.159 \times \text{Contrast} + 0.296 \times \text{Correlation} - 0.404 \times \text{Uniformity} - 0.33 \times \text{Homogeneity} + 0.41 \times \text{Entropy}$

*Principle component2:*

$0.393 \times \text{Mean} + 0.09 \times \text{Standard deviation} - 0.277 \times \text{Skewness} + 0.132 \times \text{Kurtosis} + 0.611 \times \text{Contrast} - 0.493 \times \text{Correlation} - 0.043 \times \text{Uniformity} - 0.351 \times \text{Homogeneity} + 0.021 \times \text{Entropy}$

*Elastography Index* =  $(5.304 \times \text{Prin1} + 1.937 \times \text{Prin2})/9$

Table 2 summarizes the diagnostic performances calculated using the cutoff values for each parameter. Sensitivity of grayscale index was highest, 89.3%, compared to US features and elastography index, 60.7% and 85.7%, respectively ( $p=0.005$  and  $0.002$ ). Specificity, accuracy, and PPV was highest in US features, 91.8%, 84.1%, and 70.8%, respectively, all values showing statistically significant differences when compared to grayscale US parameters (all  $ps < 0.05$ ). When comparing specificity, accuracy and PPV between grayscale US and elastography parameters, specificity and accuracy of elastography was significantly higher than grayscale US parameters, 87.1% to 64.7%, 76.1% to 62.8%, respectively ( $p < 0.001$  and  $0.022$ ). AUC value of US features was the highest, 0.762 (95% confidence interval [CI]: 0.666, 0.860), but without significant differences when compared to

the highest value among grayscale US parameters (grayscale index) or elastography parameters (mean), 0.661 (95% CI: 0.554, 0.769) and 0.645 (95% CI: 0.525, 0.766), respectively (all  $p > 0.05$ ).

### Discussion

To the present, the role of US in evaluating DTD has been limited to the detection or screening of coexisting nodular diseases or infiltrating tumors rather than providing information of the disease course.<sup>1,2,13</sup> At present, clinical or laboratory findings are considered more sensitive and accurate than US features in monitoring patients with DTD.<sup>1-3</sup> But several studies have proven US features to be useful in detecting DTD and to some extent correlates to serologic markers used in monitoring these patients.<sup>1,3,22</sup> Our results are similar to the prior reports<sup>1,3,22</sup> in that US features showed high specificity (91.8%), accuracy (84.1%), and PPV (70.8%), also with comparably higher  $A_z$  values in the diagnosis of DTD. Although US is an excellent diagnostic tool in evaluating diseases originating from the thyroid, one major limitation of US is its subjectiveness, that is, opinion may vary among radiologists in image assessment. Quantitative data such as the parameters obtained from texture analysis or elastography may be considered more objective and accurate than gross assessment of imaging features alone, but results of our study proved otherwise. Even still, we think that our results support the importance of real-time imaging and experience of the radiologist during US examinations, of which cannot be exceeded with any other software or mechanical device.

Histogram parameters which showed significant differences between patients with or without DTD in grayscale US and elastography were somewhat different; while correlation, uniformity, and entropy showed significant differences in grayscale US, mean showed significant differences in elastography. Correlation, uniformity, and entropy of co-occurrence matrix are parameters related to textural directivity, textural uniformity, and textural randomness,<sup>14,21</sup> and among grayscale US parameters, correlation and entropy showed significantly higher values in DTD while uni-

formity showed lower values (Table 1). In several other studies using texture analysis in the differential diagnosis of masses originating from various organs showed similar results,<sup>8,23-26</sup> as heterogeneous contents within the mass or desmoplastic reactions with infiltrations may cause textural heterogeneity and randomness. Common pathologic features of DTD are inflammatory infiltrations and fibrosis within the diseased parenchyma,<sup>9,14,21,27</sup> and we believe that these parameters reflect the parenchymal heterogeneity in DTD although with a lesser extent compared to cancerous processes.

Mean values were higher in elastography regardless of DTD compared to mean of grayscale US (Table 1). As the mean value represents the average pixel intensity within the ROI, this may be due to the different baseline pixels of grayscale and elastography, as the elastography images used in analysis of this study presented as multiple pixels consisting of 1 of 256 colors. Interestingly, the parameters reflecting textural heterogeneity did not show significant differences between patients with or without DTD in elastography as in the results of grayscale US parameters. Also, grayscale index showed the highest AUC value among histogram parameters of grayscale US, 0.661 (95% CI: 0.554, 0.769), while mean had the highest value among parameters of elastography, 0.645 (95% CI: 0.525, 0.766). This may be due to the dominance of mean among the histogram parameters from elastography. Elastography index is a comprehensive value representing the combination of 9 texture analysis parameters, but may not be enough to overcome the dominance of mean in elastography as shown in the results of our study.

There are several limitations to this study. First, the pathologic diagnosis of DTD was used in our study, and findings of serological marker had not been considered. During clinical practice, serologic markers are mostly used to monitor the disease course in patients with DTD, not the pathologic diagnosis, but for definitive diagnosis we had included patients who had undergone surgery. Changes in serologic markers sensitively reflect the disease course in patients with DTD, and various phases of thyroiditis can be de-

tected using these markers which had not been used in this study. Further studies correlating the serologic markers to the parameters derived from grayscale US and RTE are anticipated. Second, different measurement areas were used during data acquisition. This was inevitable since the patients included in this study were scheduled to have surgery, and had thyroid masses of variable sizes. Third, intra- or interobserver variability in obtaining elastography images had not been considered. In addition, the radiologist who performed preoperative staging US had evaluated the presence of DTD on US, in which results may have differed if multiple radiologists had been involved in image interpretation.

In conclusion, diagnostic performances were the highest for grayscale US features in diagnosis of DTD. Grayscale index may be used as a complementary tool to US features for improving sensitivity and NPV.

## Acknowledgments

This research was supported by Basic Science Research Program through the National Research Foundation of Korea (NRF) funded by the Ministry of Education (2016R1D1A1B03930375).

## References

- 1) Moon WK, Choi JW, Cho N, Park SH, Chang JM, Jang M, et al. Computer-aided analysis of ultrasound elasticity images for classification of benign and malignant breast masses. *AJR Am J Roentgenol* 2010;195(6):1460-5.
- 2) Kim I, Kim EK, Yoon JH, Han KH, Son EJ, Moon HJ, et al. Diagnostic role of conventional ultrasonography and shear-wave elastography in asymptomatic patients with diffuse thyroid disease: initial experience with 57 patients. *Yonsei Med J* 2014; 55(1):247-53.
- 3) Marcocci C, Vitti P, Cetani F, Catalano F, Concetti R, Pinchera A. Thyroid ultrasonography helps to identify patients with diffuse lymphocytic thyroiditis who are prone to develop hypothyroidism. *J Clin Endocrinol Metab* 1991;72(1):209-13.
- 4) Pedersen OM, Aardal NP, Larssen TB, Varhaug JE, Myking O, Vik-Mo H. The value of ultrasonography in predicting autoimmune thyroid disease. *Thyroid* 2000;10(3):251-9.
- 5) Moon HJ, Sung JM, Kim EK, Yoon JH, Youk JH, Kwak JY. Diagnostic performance of gray-scale US and elastography in solid thyroid nodules. *Radiology* 2012;262(3):1002-13.
- 6) Park SH, Kim SJ, Kim EK, Kim MJ, Son EJ, Kwak JY. Interobserver agreement in assessing the sonographic and elastographic features of malignant thyroid nodules. *AJR Am J Roentgenol* 2009;193(5):W416-23.
- 7) Rago T, Santini F, Scutari M, Pinchera A, Vitti P. Elastography: new developments in ultrasound for predicting malignancy in thyroid nodules. *J Clin Endocrinol Metab* 2007;92(8):2917-22.
- 8) Castellano G, Bonilha L, Li LM, Cendes F. Texture analysis of medical images. *Clin Radiol* 2004;59(12):1061-9.
- 9) Friedrich-Rust M, Ong MF, Herrmann E, Dries V, Samaras P, Zeuzem S, et al. Real-time elastography for noninvasive assessment of liver fibrosis in chronic viral hepatitis. *AJR Am J Roentgenol* 2007;188(3):758-64.
- 10) Gao S, Peng Y, Guo H, Liu W, Gao T, Xu Y, et al. Texture analysis and classification of ultrasound liver images. *Biomed Mater Eng* 2014;24(1):1209-16.
- 11) Gomez W, Pereira WC, Infantosi AF. Analysis of co-occurrence texture statistics as a function of gray-level quantization for classifying breast ultrasound. *IEEE Trans Med Imaging* 2012; 31(10):1889-99.
- 12) Itoh A, Ueno E, Tohno E, Kamma H, Takahashi H, Shiina T, et al. Breast disease: clinical application of US elastography for diagnosis. *Radiology* 2006;239(2):341-50.
- 13) Xie P, Xiao Y, Liu F. Real-time ultrasound elastography in the diagnosis and differential diagnosis of subacute thyroiditis. *J Clin Ultrasound* 2011;39(8):435-40.
- 14) Yoon JH, Yoo J, Kim EK, Moon HJ, Lee HS, Seo JY, et al. Real-time elastography in the evaluation of diffuse thyroid disease: a study based on elastography histogram parameters. *Ultrasound Med Biol* 2014;40(9):2012-9.
- 15) Mazziotti G, Sorvillo F, Iorio S, Carbone A, Romeo A, Piscopo M, et al. Grey-scale analysis allows a quantitative evaluation of thyroid echogenicity in the patients with Hashimoto's thyroiditis. *Clin Endocrinol (Oxf)* 2003;59(2):223-9.
- 16) Acharya UR, Vinitha Sree S, Mookiah MR, Yantri R, Molinari F, Zieleznik W, et al. Diagnosis of Hashimoto's thyroiditis in ultrasound using tissue characterization and pixel classification. *Proc Inst Mech Eng H* 2013;227(7):788-98.
- 17) Schiemann U, Avenhaus W, Konturek JW, Gellner R, Hengst K, Gross M. Relationship of clinical features and laboratory parameters to thyroid echogenicity measured by standardized grey scale ultrasonography in patients with Hashimoto's thyroiditis. *Med Sci Monit* 2003;9(4):MT13-7.
- 18) Loy M, Cianchetti ME, Cardia F, Melis A, Boi F, Mariotti S. Correlation of computerized gray-scale sonographic findings with thyroid function and thyroid autoimmune activity in patients with Hashimoto's thyroiditis. *J Clin Ultrasound* 2004; 32(3):136-40.
- 19) Kim SY, Kim EK, Moon HJ, Yoon JH, Kwak JY. Application of texture analysis in the differential diagnosis of benign and malignant thyroid nodules: comparison with gray-scale ultrasound and elastography. *AJR Am J Roentgenol* 2015;205(3): W343-51.
- 20) Kim EY, Kim WG, Kim WB, Kim TY, Kim JM, Ryu JS, et al. Coexistence of chronic lymphocytic thyroiditis is associated with lower recurrence rates in patients with papillary thyroid carcinoma. *Clin Endocrinol (Oxf)* 2009;71(4):581-6.
- 21) Wang J, Guo L, Shi X, Pan W, Bai Y, Ai H. Real-time

- elastography with a novel quantitative technology for assessment of liver fibrosis in chronic hepatitis B. Eur J Radiol* 2012; 81(1):e31-6.
- 22) Willms A, Bieler D, Wieler H, Willms D, Kaiser KP, Schwab R. *Correlation between sonography and antibody activity in patients with Hashimoto thyroiditis. J Ultrasound Med* 2013; 32(11):1979-86.
  - 23) Emblem KE, Nedregaard B, Nome T, Due-Tønnessen P, Hald JK, Scheie D, *et al.* *Glioma grading by using histogram analysis of blood volume heterogeneity from MR-derived cerebral blood volume maps. Radiology* 2008;247(3):808-17.
  - 24) Ganeshan B, Abaleke S, Young RC, Chatwin CR, Miles KA. *Texture analysis of non-small cell lung cancer on unenhanced computed tomography: initial evidence for a relationship with tumour glucose metabolism and stage. Cancer Imaging* 2010; 10:137-43.
  - 25) Ganeshan B, Skogen K, Pressney I, Coutroubis D, Miles K. *Tumour heterogeneity in oesophageal cancer assessed by CT texture analysis: preliminary evidence of an association with tumour metabolism, stage, and survival. Clin Radiol* 2012; 67(2):157-64.
  - 26) Sivaramakrishna R, Powell KA, Lieber ML, Chilcote WA, Shekhar R. *Texture analysis of lesions in breast ultrasound images. Comput Med Imaging Graph* 2002;26(5):303-7.
  - 27) Sandrin L, Fourquet B, Hasquenoph JM, Yon S, Fournier C, Mal F, *et al.* *Transient elastography: a new noninvasive method for assessment of hepatic fibrosis. Ultrasound Med Biol* 2003;29(12):1705-13.